JMEPEG (2008) 17:908–914
DOI: 10.1007/s11665-008-9235-3

1059-9495/$19.00

# Microstructure and Oxidation Characteristics of Laser and GTAW Weldments in Austenitic Stainless Steels

*S.K. Samanta, S.K. Mitra, and T.K. Pal*

*(Submitted March 27, 2007; in revised form March 15, 2008)*

**The present investigation reports microstructure and high-temperature oxidation behavior of GTAW and laser weldments of 316L stainless steel. The microstructure and oxidation behavior of composite laser weldment are found to be influenced by the welding speed. In GTAW weldment, weld metal shows higher oxidation rate as compared to base metal of same weldment. Furthermore, the inoculation of Ce in GTAW weld influences the microstructure and oxidation characteristics. The scale morphologies, scale adherence, and spallation have been characterized by SEM and EDAX.**

**Keywords** austenitic stainless steel, laser weldments, oxidation rate, rare earth metal, scale morphology, weld metal

## 1. Introduction

The present investigation deals with a study on microstructural variation due to laser welding speed and GTAW welding of 316L stainless steel with weld inoculation and also their effect on oxidation resistance. The oxidation study of laser welding and inoculated GTAW welds is a new approach in this study. A new technique of doping the weld metal with rare earth metal (REM) is introduced in this experiment to modify the weld metal characteristics.

Microstructural changes due to welding have been reported to influence the oxidation rate particularly by those elements that involve an effective depletion (Ref 1, 2). However, no systematic studies have yet been reported except some from this laboratory (Ref 3, 4). This investigation presents the results on microstructural variation in weld metal doped with Ce and their effect on oxidation resistance. Inoculation with REM in GTAW weldment has been observed to suppress the columnar grains resulting in fragmentation of structure (Ref 5), which ultimately improves the oxidation resistance as well as scale adherence of 316L weldments.

This has special relevance to the applications of such steel in nuclear-power programs as potential materials for construction of primary circuit, control rod components, thermal insulation and hotbox components etc. in the fast breeder reactor.

**S.K. Samanta**, Research & Control laboratory, Alloy Steels Plant, SAIL, Durgapur 713208, India; **S.K. Mitra**, Metallurgical and Materials Engineering Department, National Institute of Technology, Durgapur 713209, India; and **T.K. Pal**, Metallurgical Engineering Department, Jadavpur University, Kolkata 700032, India. Contact e-mail: sisirsamanta@sancharnet.in.

## 2. Experimental Details

In the present study, AISI 316L materials in the form of 100×50×6 mm plates have been procured in annealed condition. The chemical composition of 316L and filler metal are given in Table 1.

The joint preparation for laser welding has been done by machining on both edges to make square butt joints. The laser welding has been carried out in 5 kW $CO_2$ laser with two different travel speeds. In case of GTAW welding, joint preparation is done by machining on both edges to make single 'V' groove shape having included angle of 90°. GTAW welding has been carried out in Master TIG MLS 2500 kemppi make machine and welding was completed in three passes (two front passes and 1 back pass after gouging). Cerium has been introduced into the weld metal with the help of specially made filler rod filled with Ce in the form of Misch metal (having 50% Ce). Transverse sections of the welded samples are polished, cleaned, and etched with aqua regia ($HNO_3$:HCl 1:3) for examining the microstructural constituents by scanning electron microscope (SEM). Ferrite measurement has been done by using MagneGage, which is calibrated by no 3 magnet in accordance with the procedure in AWS A 4.2-74. Welding parameters are summarized in Tables 2 and 3.

Oxidation of GTAW and laser-welded specimens has been carried out in a muffle furnace at 973 K for a period of 240 h. The weight gains of base metal and weld metal of GTAW weldments and also the laser-welded (with variation of speed) composites under similar oxidizing condition have been measured by means of an electronic digital balance of accuracy of ±0.01 mg. The microstructure has been characterized by SEM LEO S 430 I, U.K., coupled with Link ISIS EDX detector.

## 3. Results and Discussion

Many authors (Ref 6-8) have observed changes in microstructure in case of laser welds. The laser welds in the present

**Table 1 Chemical composition**

| Material | C | Mn | P | S | Si | Cr | Mo | Ni | Al | $N_2$ (ppm) |
|---|---|---|---|---|---|---|---|---|---|---|
| 316L | 0.025 | 1.87 | 0.039 | 0.019 | 0.30 | 16.8 | 2.12 | 10.6 | 0.014 | 190 |
| Filler for GTAW | 0.022 | 1.35 | 0.031 | 0.014 | 0.28 | 17.0 | 2.10 | 11.52 | 0.017 | 180 |

**Table 2 Laser welding parameters**

| Welding speed, mm/s | Laser power, kW | Voltage, V | Current, A | Focusing point inside material, mm | Shielding gas |
|---|---|---|---|---|---|
| 11.66<br>25 | 3 | 110 | 20 | 1 | Argon |

**Table 3 GTAW welding parameters**

| Voltage, V | Current, A | Welding speed, mm/s | Interpass temperature, K |
|---|---|---|---|
| 11–12 | 90–96 | 0.63–0.74 | 423 |

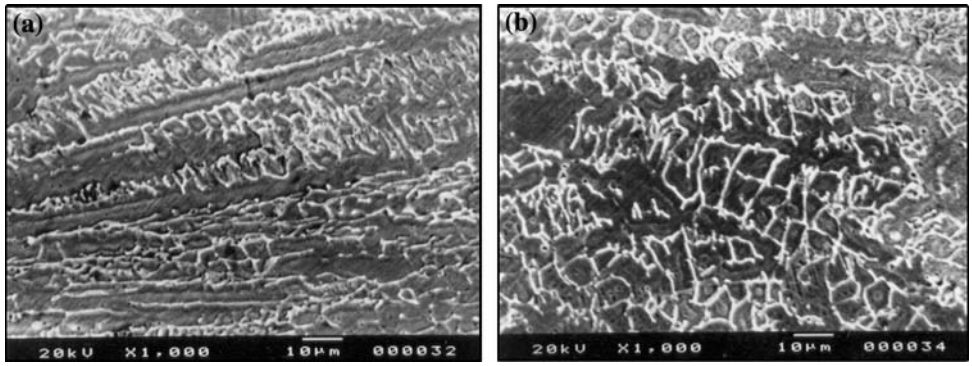


**Fig. 1** SEM of 316L laser weldments at 11.66 mm/s: (a) near fusion boundary and (b) center

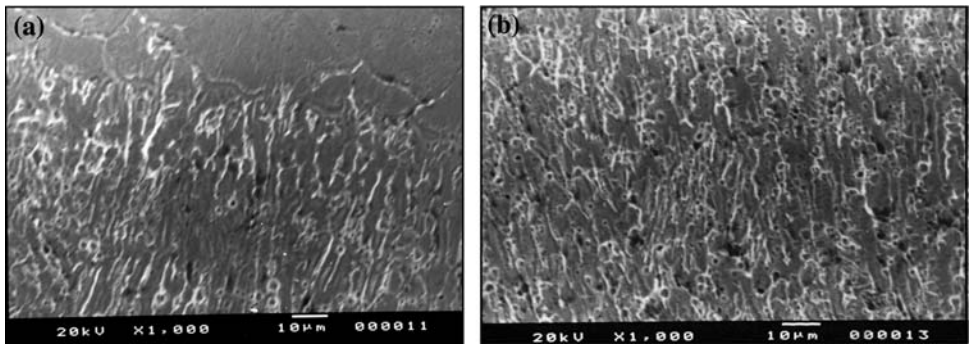


**Fig. 2** SEM of 316L laser weldments at 25 mm/s: (a) near fusion boundary and (b) center

work consist of duplex microstructure, i.e., austenite plus ferrite. The changes are noticed in this work not only with speed but also with the position in the weld bead. At lower speed (11.66 mm/s), mixed ferrite morphology of lacy and vermicular has been observed near the fusion boundary and predominantly vermicular ferrite near the center (Fig. 1). On the other hand, cellular austenite and some amount of ferrite have been observed near fusion boundary and also at the center (Fig. 2) at higher speed (25 mm/s).

The increase or decrease in ferrite content of austenitic stainless steel weld metal is considered to be associated with decrease or increase in solidification rates respectively as the solidification rates have been observed to have a pronounced effect on the ferrite content of the metal (Ref 9-11).

In case of GTAW weld, duplex microstructure has also been revealed with some directionality only near fusion boundary. However, such directionality is absent at the center region. This has been observed both with and without cerium doping. This behavior may be due to local variation in solidification mode and growth velocity at fusion boundary and center position of the weld (Ref 12). Addition of Ce not only refines the structure but also decreases the ferrite

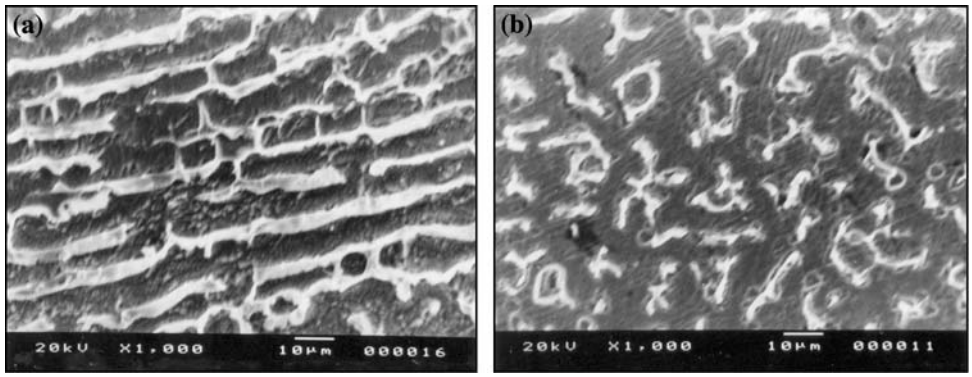


**Fig. 3** SEM of 316L GTAW weldments with 0.03% Ce: (a) near fusion boundary and (b) center

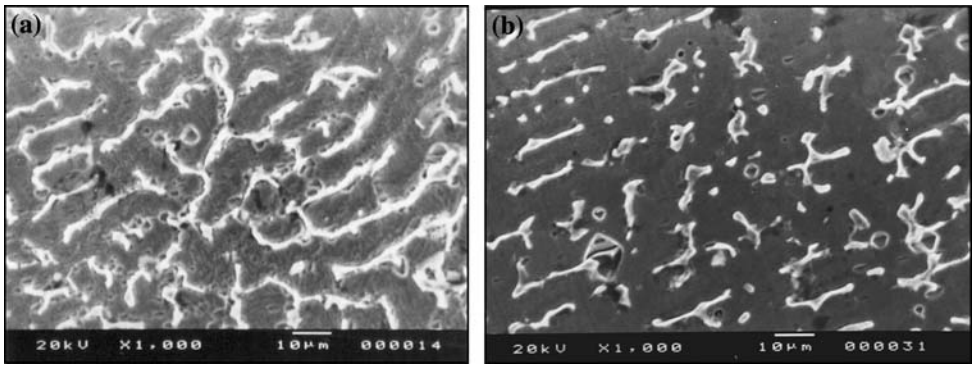


**Fig. 4** SEM of 316L GTAW weldments with 0.08% Ce: (a) near fusion boundary and (b) center

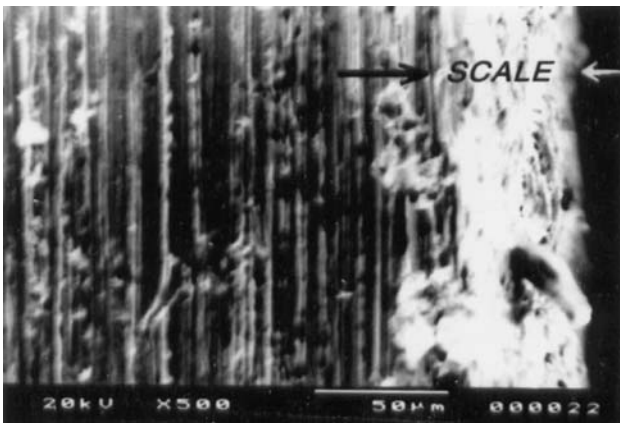


**Fig. 5** Cross-sectional view of 316L weldment after oxidation showing inner and outer scale

content with increase in Ce content from 0.03(FN 7) to 0.08 (FN 5) (Figs. 3 and 4).

The oxide scale of base metal (316L) shows fine grains near alloy/scale interface and a stratified layer at scale/air interface (outside of the scale) (Fig. 5). After removing the oxide scale, the microstructure shows predominant growth of dendrites in center as well as near fusion boundary (Fig. 6). The composite laser weldment, consisting mainly of weld metal and base metal of 316L, is found to have higher oxidation rate when joined with lower welding speed of 11.66 mm/s as compared to 25 mm/s (Fig. 7).

Slower welding speed causes Cr enrichment at the fusion boundary, whereas Cr enrichment peak shifts to weld metal at higher welding speed as shown in Fig. 8. Therefore, depletion of Cr content in the matrix as well as in the inner scale has been considerably lower at lower speed than at higher speed, since Cr is the main corrosion-resisting element of austenitic stainless steels. This caused more mass gain per unit area during subsequent oxidation of laser-welded 316L SS (Fig. 7) at welding speed of 11.66 mm/s.

Furthermore, a lower Cr content renders the scale less protective by facilitating the diffusion of the species involved in oxidation processes. On the other hand, in case of high-speed weldments most of the Cr is available for formation of protective scale and hence improves the oxidation resistance.

The SEM of the oxidized samples shows a change in scale morphology due to change in laser welding speed (Fig. 9a and b).

EDX spectrum of the top scale (scale/air layer) exhibits mainly iron oxide with oxides of Cr, Mn, and Ni (Fig. 10a and b). The oxide particles are smaller in size and nodular in shape. Clustering of oxide grains having definite geometrical shapes have been observed at some locations in weld metal zone (Fig. 9a). At higher speed, the oxide nodules have no definite shape and are coarser than specimen at lower welding speed, but do not form cluster zones (Fig. 9b).

EDX spectrum of the top scales clearly shows the variation in composition due to two differentially maintained welding

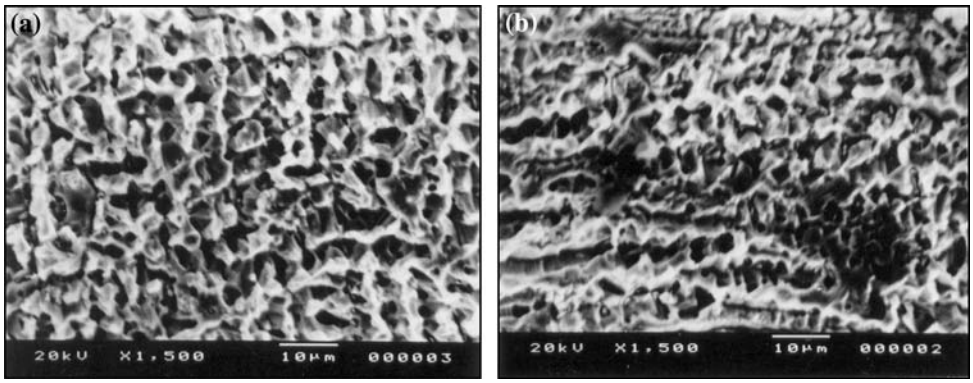


**Fig. 6** SEM of 316L weldments after oxidation showing growth of dendrites: (a) center and (b) near fusion boundary

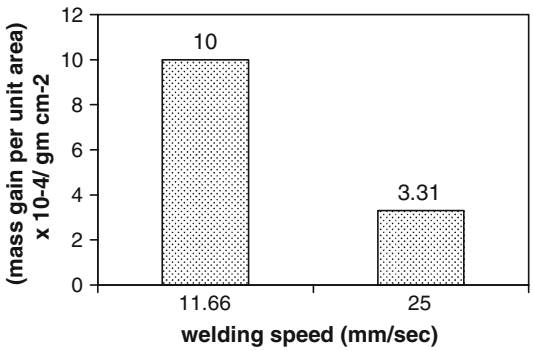


**Fig. 7** Oxidation of laser weldments at different speeds

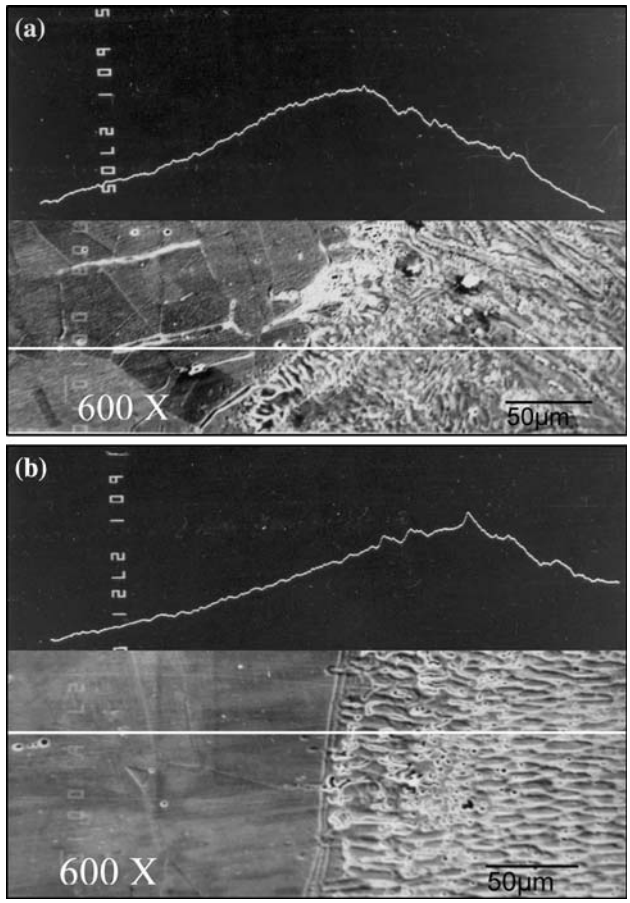


**Fig. 8** EPMA concentration profile for Cr at different speeds: (a) at 1166 mm/s and (b) at 25 mm/s

speeds (Fig. 10a and b). The average Fe/Cr ratio of top scale for 11.66 and 25 mm/s are 3.5 and 3.0, respectively. EDX analysis of inner scale adhering to the alloy surface after removing the top scales exhibits the Fe/Cr ratio 4.0 and 3.4 for the welding speed 11.66 and 25 mm/s, respectively. The average element analysis of the inner scale shows 11.24% Cr and 13.24% Cr content, respectively.

It is observed from SEM that the pretreatment of 316L stainless steel by laser welding with different speed has a significant role in the subsequent oxidation process and oxide scale morphologies (Ref 13-16). This effect is due to the change in Cr concentration profile of the base metal zone with the variation in welding speed. The heating intensity and subsequent cooling rate are the major factors for such variation in composition (Ref 5). The SEM of oxidized GTAW weld metal cross section shows a more compact inner (alloy/scale) layer than outer scale/air layer. The outer (scale/air) layer has tendency to cracking and spalling of the scale during cooling of the specimen (Fig. 11).

Again, there is a distinct difference in scale morphologies between base metal and weld metal of GTAW welded 316L stainless steel specimen oxidized at 973 K for 240 h (Fig. 12a and b). The mass gain per unit area of the weld metal has been found to be 45% higher than the base metal zone of the 316L weldment. Higher mass gain means a thicker scale has formed over weld metal during oxidation process and this is generally more prone to cracking during cooling process (Fig. 11). Chromium content near the inner boundary of the oxide scales formed over weld metal has been found to be higher (i.e., Fe/Cr ratios are significantly higher) than those formed over base metal (Fig. 13a and b).

The oxidation resistance properties of weld metal were improved by misch metal doping (addition of Ce). The SEM of the top scale of cerium-doped weld metal shows fine nodular-shaped grains (Fig. 14) as compared to large needle-shaped oxide grains on the undoped weld metal (Fig. 12b).

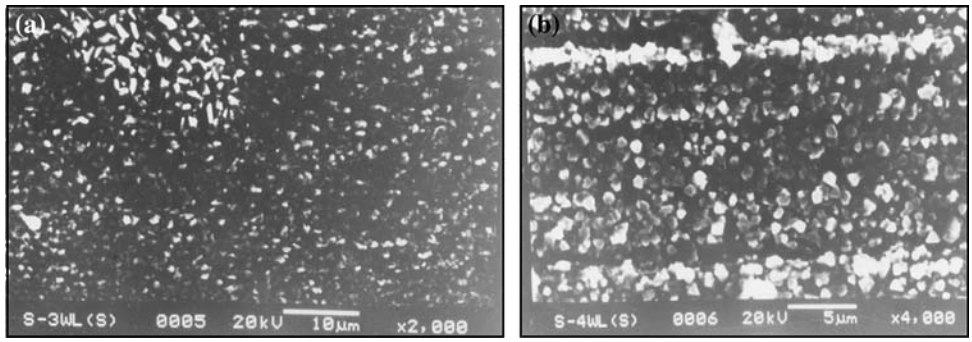


**Fig. 9** SEM of oxidized weldments showing change in scale morphology at different speeds: (a) at 11.66 mm/s and (b) 25 mm/s

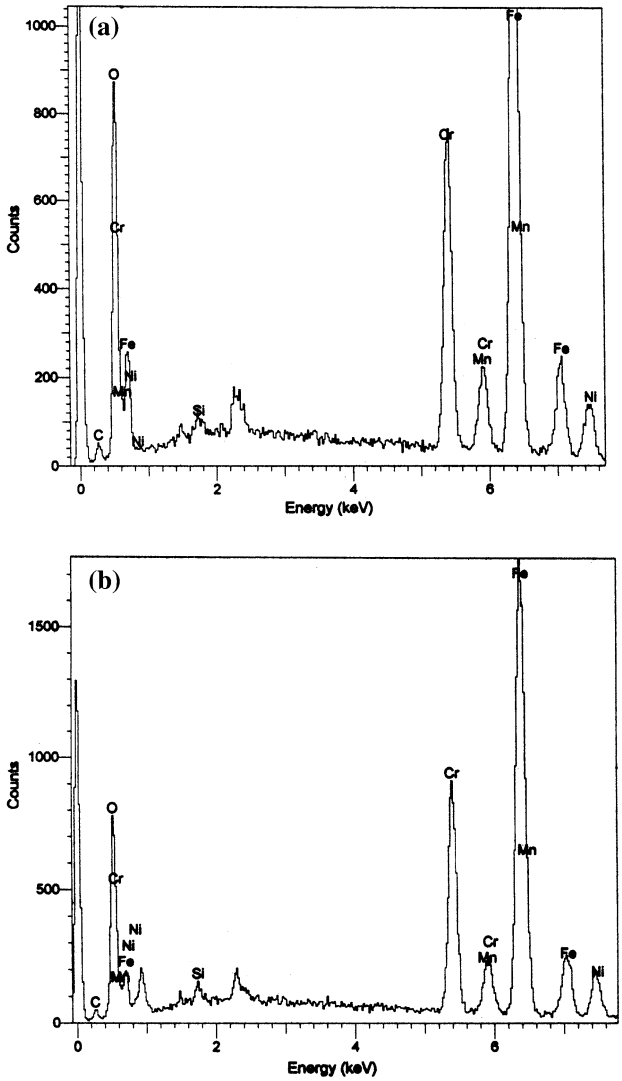


**Fig. 10** EDX of 316L weldment top scale formed over weld metal zone: (a) 11.66 mm/s and (b) 25 mm/s

Significant improvement in mass gain per unit area of misch metal-doped weld metal zone has been observed as shown in Fig. 15. The presence of cerium in the form of oxides $Ce_2O_3$, CeO, and $CeFeO_3$ in the weld metal could be the main reason for the prevention of subsequent scale growth process which resulted in excellent oxidation resistance of 316L SS weldment as indicated in Fig. 15.

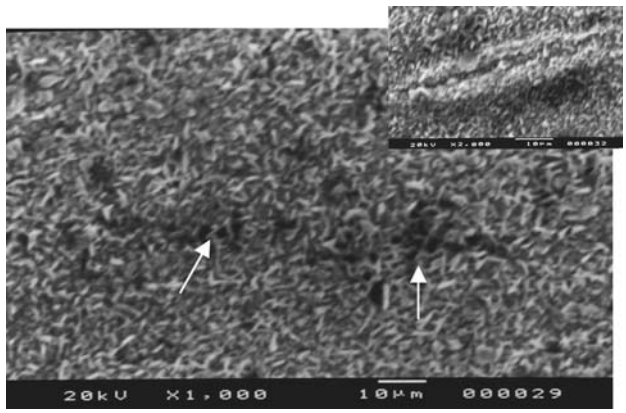


**Fig. 11** Top scale showing cracking (with magnified view)

## 4. Conclusion

The following conclusions may be drawn from the present study:

1. Variation in microstructure and ferrite morphology of the laser weldment is found to be influenced by the welding speed.
2. Mass gain per unit area of the laser weldment decreases with increasing welding speed. Total oxidation of the composite weldment has decreased to 67% with increase in welding speed from 11.66 to 25 mm/s.
3. In GTAW weld, the microstructure near fusion boundary shows directionality but no such directionality has been noted at the center.
4. A considerably thicker scale has formed over the weld metal zone as compared to those on the base metal of the 316L GTAW weldment.
5. Cerium doping in weld metal resulted in an improvement in the oxidation resistance of the weld metal.

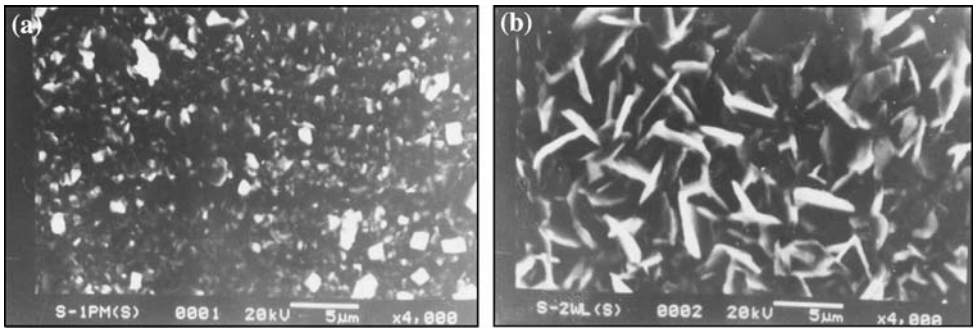


**Fig. 12** SEM of 316L top scale morphologies: (a) base metal and (b) weld metal

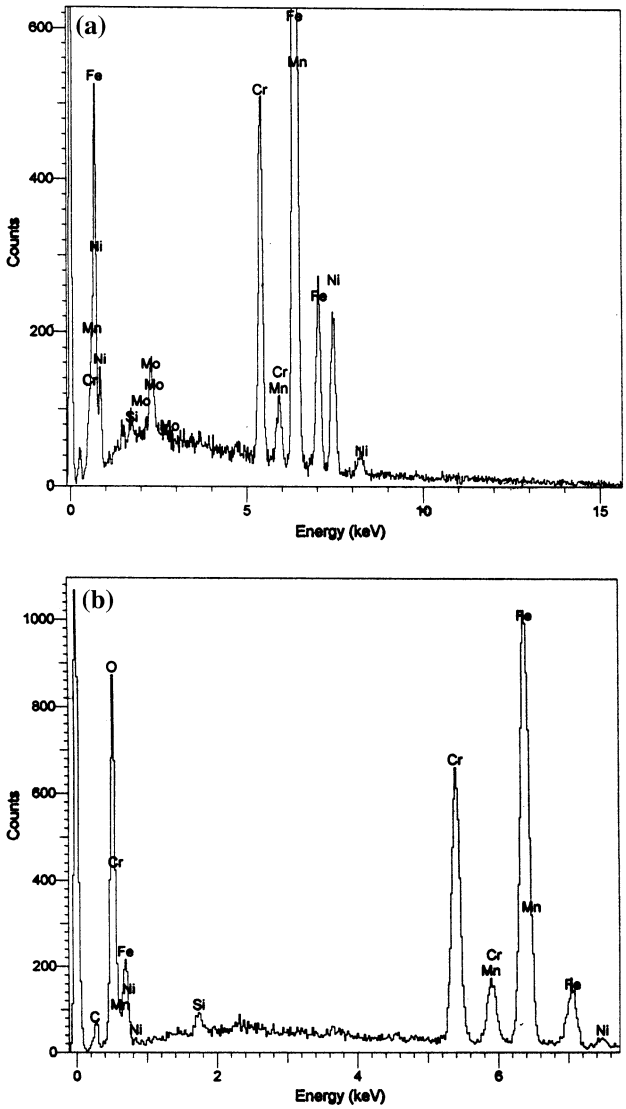


**Fig. 13** EDX of 316L top scale formed over (a) base metal and (b) weld metal

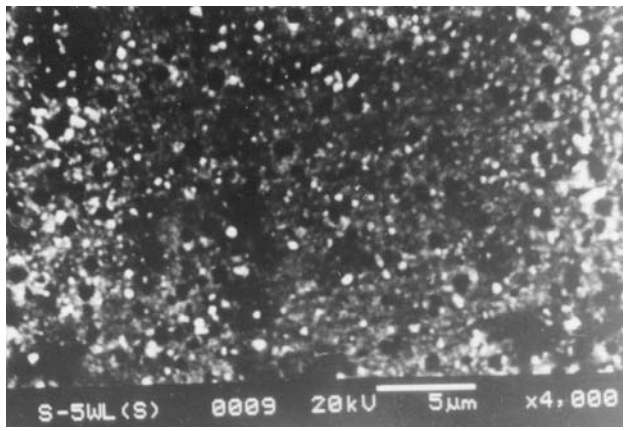


**Fig. 14** SEM of the top scale of cerium-doped weld metal

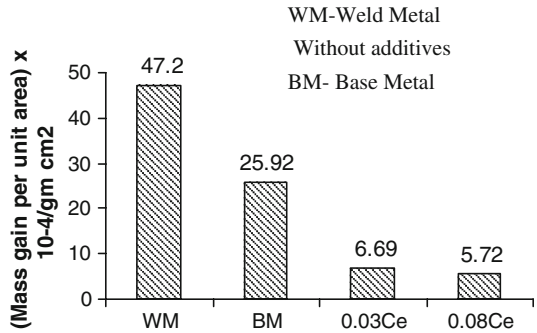


**Fig. 15** Oxidation rate of various weld zones and base metal of 316L oxidized at 973 K in $PO_2$ = 21.27 kPa for 240 h

## References


1. R.K. Singh Raman, A.S. Khanna, and J.B. Gyanamoorthy, Effect of Tempering Time on the Oxidation Behaviour of 2¼Cr-1Mo Steel, *Oxid. Met.*, 1988, **30**, p 345
2. R.K. Singh Raman and J.B. Gyanamoorthy, Oxidation Behaviour of 2¼Cr-1Mo Steel with Prior Tempering Treatments at 998 K for Different Durations, *J. Mater. Sci.*, 1992, **27**, p 3435
3. S.K. Mitra, S.K. Roy, and S.K. Bose, Influence of a Mixed $Al_2O_3$ + $Cr_2O_3$ Superficial Coating on the Non-Isothermal Oxidation Behavior of Fe and Fe-Cr alloys, *Oxid. Met.*, 1992, **37**, p 95
4. S.K. Samanta, S K Mitra, and T.K. Pal, Influence Of Welding Speed on Microstructure and Oxidation Behaviour of Laser Welded Austenitic Stainless Steels, *ISIJ Int.*, 2006, **46**(1), p 100–105
5. A.B. Geller and O.S. Kakovkin, Metallurgical Features of Reduction of Rare Earth Metals from their Oxides in Welding with Coated Electrodes, *Weld. Prod.*, 1986, **10**, p 30–32
6. N. Suutala, T. Takalo, and T. Moisio, Single Phase Ferritic Solidification Mode in Austenitic Ferritic Stainless Steel Welds, *Met. Trans. A*, 1979, **10A**(8), p 1183–1190

7. Y. Arata, F. Matsuda, and S. Katyama, Solidification Crack Susceptibility in Weld Metals of Fully Austenitic Stainless Steels (Report II) – Effect of Ferrite, P, S, C, Si and Mn on Ductility Properties of Solidification Brittleness, *Trans. JWRI*, 1977, **6**, p 105–116
8. S. David, J. Vitek, and T. Hebble, Effect of Rapid Solidification on Stainless Weldment Microstructure and its Implications on the Scaeffler Diagram, *Weld. J.*, 1987, **66**(10), p 289s–300s
9. T.P.S. Gill, M. Vijayalakhmi, J.B. Gnanamoorthy, and K.A. Padmanabhan, Transformation of Delta Ferrite during Post Weld Treatment of Type 316L Steel Weld Metal, *Weld. J.*, 1986, **May**, p 122s–128s
10. S. Venkataraman and J. Develetian, Rapid Solidification of SS by Capacitor Discharge Welding, *Weld. J.*, 1988, **67**(6), p 111s–118s
11. H. Inoue, T. Koseki, S. Okhita, and T. Tanaka, Effect of Solidification and Subsequent Ferrite to Austenite Massive Transformation in an Austenitic SS Weld Metal, *ISIJ Int.*, 1995, **35**(10), p 1248–1257
12. N. Sutala, T. Takalo, and T. Moisio, Ferritic-Austenitic Solidification Mode in Austenitic Stainless Steel Welds, *Met. Trans. A*, 1980, **11A**, p 717–725
13. R.K. Singh Raman and J.B. Gyanamoorthy, Oxidation Behavior of Weld Metal, HAZ and Base Metal Regions in Weldments of Cr-Mo Steels, *Weld. Res.*, 1995, **Supplement**, p 133–138
14. K. Easterling, *Introduction to Physical Metallurgy of Welding*, Butterworth, 1983
15. D. Lundin, Structure & Properties of Weldments, *Proc. Advance in Welding Science and Technology*, S.A. David, Ed., ASM International, 1988
16. U.K. Chatterjee, S.K. Bose, and S.K. Roy, *Enviromental Degradation of Metals*. Marcel Dekker, Inc., New York, 2001, p 70–73